ARCHIVES OF MECHANICS
Arch. Mech. **72** (2), 81–107, 2020, DOI: 10.24423/aom.3268

An analytical study on the nonlinear forced vibration of functionally graded carbon nanotube-reinforced composite beams on nonlinear viscoelastic foundation

H. SHAFIEI, A. R. SETOODEH

Department of Mechanical and Aerospace Engineering, Shiraz University of Technology, Shiraz 71555, Iran, e-mails: setoodeh@sutech.ac.ir, asetood@yahoo.com

This paper deals with the nonlinear forced vibration of nanocomposite beams resting on a nonlinear viscoelastic foundation and subjected to a transverse periodic excitation. It is considered that the functionally graded carbon nanotube-reinforced composite (FG-CNTRC) beam is made of an isotropic matrix reinforced by either aligned- or randomly oriented-straight single-walled carbon nanotubes (SWCNTs) with four types of distributions through the thickness direction of the beam. Both the Eshelby–Mori–Tanaka approach and extended rule of mixtures are used to predict the effective material properties of the FG-CNTRC beams. The mathematical model of the beam is developed based on the Euler–Bernoulli beam theory together with von Kármán assumptions. Subsequently, the accurate analytical solutions of the governing equation are obtained through applying the variational iteration method (VIM). Several examples are verified to have higher accuracy than those available in the literature. In addition, a comprehensive investigation into the effect of carbon nanotubes (CNTs) distribution, CNTs volume fraction, end supports, vibration amplitude, and foundation coefficients on the vibrational characteristics of the nanocomposite beam is performed and some new results are presented.

Key words: nonlinear forced vibration, nanocomposite beams, functionally graded materials, nonlinear viscoelastic foundation.

1. Introduction

The concept of functionally graded materials (FGMs) was first introduced by a group of Japanese scientists in 1984 [1, 2]. FGMs are inhomogeneous composite materials and characterized by a smooth and continuous variation of material properties in one or more directions over volume. Due to remarkable thermal and mechanical properties of FGMs, their applications have been rapidly increased in different fields of science and industries and consequently, many investigators studied the mechanical properties of different structures made of FGMs [3–6]. Among all of the structural elements, FGM beams are of significant importance and have been widely studied by researchers [7–10].

By development of nanotechnology and emergence of carbon nanotubes [11], many studies were conducted on the mechanical properties of the novel nanoscale materials, and particularly CNTs [12–14]. It was reported that, in addition to the exceptional electrical and mechanical properties of CNTs, they are suitable materials to be used as reinforcement phase in composite materials including FGMs [15]. Thus, examining the mechanical behavior of carbon nanotube-reinforced composite structures has been provided extensive opportunities for scientists in various research areas [16–24]. Meanwhile, free vibration and buckling of CNTRC beams resting on an elastic foundation were studied in the context of Timoshenko beam theory by Yas and Samadi [25]. They employed the generalized differential quadrature method to solve the related equation. Wu *et al.* [26] studied the nonlinear free vibration of a geometrically imperfect FG-CNTRC beam utilizing the first-order shear deformable theory. The imperfections were described using a model consisting of trigonometric and hyperbolic functions. Free vibration analysis of FG-CNTRC beams in thermal environment was examined by Shenas *et al.* [27]. They assumed that the beam is pre-twisted and showed that fundamental frequency parameters enhance by increasing the pre-twist angle. Based on the first-order shear deformation theory, Vo-Duy *et al.* [28] investigated the free vibration of laminated FG-CNTRC beams. They considered different distribution of SWCNTs in each layer of the nanocomposite beam.

Among all of the investigations cited thus far, less attention has been attracted to the forced vibration analysis of FG-CNTRC structures. For the case of beams, Yas and Heshmati [29] employed both the Euler–Bernoulli and Timoshenko beam theories to discuss the linear forced vibration of FG nanocomposite beams reinforced by randomly oriented CNTs subjected to a moving load. The material properties of the CNTRC beam were evaluated using the Eshelby–Mori–Tanaka approach. Through utilizing the Timoshenko beam theory and von Kármán geometric nonlinearities together with a differential quadrature method, the nonlinear forced vibration of FG-CNTRC Timoshenko beams was studied by Ansari *et al.* [30]. Wu *et al.* [31] examined the nonlinear primary and superharmonic resonances of FG-CNTRC beams. They derived coupled equations of motion by means of the Hamilton principle and Galerkin technique and employed the incremental harmonic balance method to solve the equations.

Foundations are important parts of physical systems due to their wide range of applications in different science and engineering areas [32]. Viscoelastic foundations are among the most practical and realistic models and several researchers have employed them to examine mechanical behavior of real structures. For instance, Chen *et al.* [33] studied the dynamic response of an infinite or semi-finite beam on viscoelastic foundation subjected to harmonic moving load for the railway engineering applications. A nonlinear viscoelastic foundation was applied by Bhattiprolu *et al.* [34] to model restoring force of flexible polyurethane foams, which are used in furniture and automotive industry.

By a comprehensive review of the literature, it was found that most of the researchers have considered aligned and straight CNTs as reinforcements of nanocomposite beams and have determined material properties of these structures using the extended rule of mixture. In this study, in addition to the aligned CNTs, it is assumed that CNTs are randomly oriented in the polymeric matrix. Thus, the Eshelby–Mori–Tanaka approach, which is applicable in both cases of aligned- and randomly oriented-straight CNTs, is also employed to calculate the effective material properties of the FG-CNTRC beams. The CNTs are graded gradually in the thickness direction of the beam with different distributions. The beam is subjected to a transverse periodic excitation and is resting on a nonlinear viscoelastic foundation. Based on the Euler–Bernoulli beam theory and Hamilton's principle, the governing equation of the nanobeam is developed. The variational iteration method is applied to solve the nonlinear governing equation and the closed form solutions are provided for the vibrational behavior of the nanocomposite beam. To the best of authors' knowledge, no analytical results have been reported in the literature for nonlinear forced vibration analysis of FG-CNTRC beams reinforced by randomly oriented CNTs. The developed results in this paper reveal the influences of different parameters on the nonlinear frequencies and vibration response of the nanobeams.

2. Effective material properties of FG-CNTRC beam

In this work, straight SWCNTs parallel to the longitudinal direction of the beam and straight SWCNTs randomly oriented in different directions are selected as the reinforcements of the CNTRC beams. Two different approaches as the Eshelby–Mori–Tanaka (EMT) and the extended rule of mixture (ERM) are employed to estimate the material properties of the CNTRC beams. The EMT can be utilized for nanocomposites reinforced with either aligned or randomly oriented CNTs [35]. However, the ERM is applicable only when the straight CNTs are aligned in the matrix [36].

2.1. Extended rule of mixture

The effective Young's and Shear moduli of the CNTRC with aligned CNTs along the longitudinal direction are predicted using the ERM as follows [36]:

$$E_{11} = \eta_1 V^{cnt} E_{11}^{cnt} + V_m E_m, \tag{2.1a}$$

$$\frac{\eta_2}{E_{22}} = \frac{V^{cnt}}{E_{22}^{cnt}} + \frac{V_m}{E_m}, \tag{2.1b}$$

$$\frac{\eta_3}{G_{12}} = \frac{V^{cnt}}{G_{12}^{cnt}} + \frac{V_m}{G_m}, \tag{2.1c}$$

where E_{11}^{cnt}, E_{22}^{cnt} and G_{12}^{cnt} are the Young's and shear moduli of CNTs, respectively. E_m and G_m denote the corresponding material properties of the isotropic matrix. η_i $(i = 1, 2, 3)$ are the CNTs efficiency parameters stating the size-dependent material properties and are calculated through equalizing the elastic moduli results assessed from the molecular dynamics (MD) simulations [16] to the counterparts evaluated from the ERM. V_m and V^{cnt} are the volume fractions of the matrix and CNTs, respectively, and are related by $V^{cnt} + V_m = 1$. Similarly, the effective Poisson ratio ν_{12} and the mass density ρ of the CNTRC beam can be determined as:

$$\nu_{12} = V^{cnt}\nu_{12}^{cnt} + V_m\nu_m, \qquad \rho = V^{cnt}\rho^{cnt} + V_m\rho_m. \tag{2.2}$$

The considered distribution patterns of CNTs in the matrix, depicted in Fig. 1, are in the form of:

$$\text{UD: } V^{cnt} = V_*^{cnt}, \tag{2.3}$$

$$\text{FGA: } V^{cnt} = \left(1 + \frac{2z}{h}\right)V_*^{cnt}, \tag{2.4}$$

$$\text{FGX: } V^{cnt} = 4\frac{|z|}{h}V_*^{cnt}, \tag{2.5}$$

$$\text{FGO: } V^{cnt} = \left(2 - 4\frac{|z|}{h}\right)V_*^{cnt}, \tag{2.6}$$

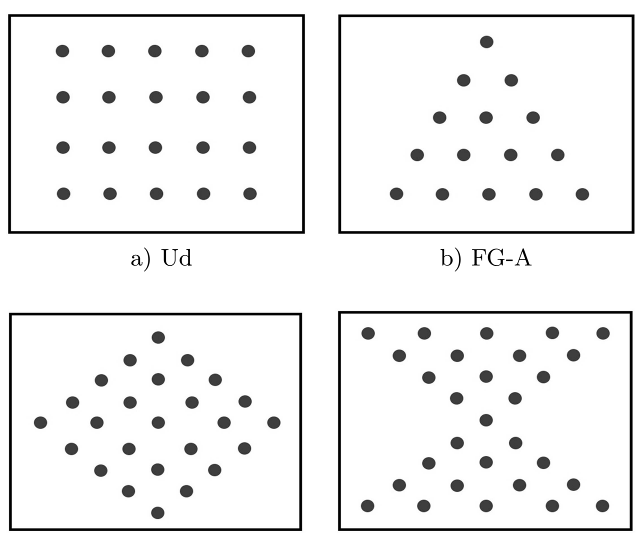

a) Ud b) FG-A

c) FG-O db) FG-X

Fig. 1. Distribution patterns of SWCNTs in the FG-CNTRC beams.

where

$$V_*^{cnt} = \frac{\Lambda^{cnt}}{\Lambda^{cnt} + \left(\frac{\rho^{cnt}}{\rho_m}\right)(1 - \Lambda^{cnt})} \tag{2.7}$$

in which Λ^{cnt} is the mass fraction of CNTs.

2.2. Eshelby–Mori–Tanaka approach

The Eshelby–Mori–Tanaka is an efficient method for evaluating the effective material properties of composites and nanocomposites while its accuracy has motivated researchers to employ it in their investigations. Moreover, there are studies that have demonstrated the correctness of this method [37,38]. The main idea of the EMT approach, also called the equivalent inclusion-average stress method, is extracted from the concept of average stress in the matrix presented by Mori and Tanaka [39] and the equivalent elastic inclusion idea of Eshelby [40].

To estimate the material properties of CNTRC beams, each CNT in the polymeric matrix is modeled by an equivalent long fiber with transversely isotropic elastic properties. Thus, the resulted composite is also transversely isotropic. Employing an equivalent fiber approach together with the numerical results obtained from MD simulations [16], the material properties of the equivalent fiber are determined.

2.2.1. Composites reinforced with aligned-straight CNTs. A composite beam reinforced with straight CNTs aligned in the x direction is considered. The material properties of the CNTRC beam can be expressed in terms of engineering constants as [41]

$$\begin{gathered} E_{11} = n - \frac{l^2}{k}, \quad E_{22} = \frac{4m(kn - l^2)}{kn - l^2 + mn}, \quad \nu_{12} = \nu_{13} = \frac{l}{2k}, \\ \nu_{23} = \frac{n(k-m) - l^2}{n(k+m) - l^2}, \quad G_{12} = G_{13} = p, \end{gathered} \tag{2.8}$$

where n, l, k, m, and p are Hill's elastic moduli of the composite; n is the uniaxial tensile modulus in the CNT direction,l is the associated transverse modulus, k is the plain-strain bulk modulus normal to the CNT direction, m and p are the shear moduli in the planes normal and parallel to the CNT direction, respectively. Based on the EMT approach, the Hill's elastic moduli of the composite beam can be described as [35]

$$k = \frac{E_m\{E_m V_m + 2k_r(1+\nu_m)[1+V^{cnt}(1-2\nu_m)]\}}{2(1+\nu_m)[E_m(1+V^{cnt}-2\nu_m)+2V_m k_r(1-\nu_m-2\nu_m^2)]}, \tag{2.9}$$

$$l = \frac{E_m\{V_m\nu_m[E_m+2k_r(1+\nu_m)]+2V^{cnt}l_r(1-\nu_m^2)\}}{(1+\nu_m)[2V_mk_r(1-\nu_m-2\nu_m^2)+E_m(1+V^{cnt}-2\nu_m)]}, \tag{2.10}$$

$$n = \frac{E_m^2V_m(1+V^{cnt}-V_m\nu_m)+2V_mV^{cnt}(k_rn_r-l_r^2)(1+\nu_m)^2(1-2\nu_m)}{(1+\nu_m)\{2V_mk_r(1-\nu_m-2\nu_m^2)+E_m(1+V^{cnt}-2\nu_m)\}} + \frac{E_m[2V_m^2k_r(1-\nu_m)+V^{cnt}n_r(1-2\nu_m+V^{cnt})-4V_ml_r\nu_m]}{2V_mk_r(1-\nu_m-2\nu_m^2)+E_m(1+V^{cnt}-2\nu_m)}, \tag{2.11}$$

$$p = \frac{E_m[E_mV_m+2p_r(1+V^{cnt})(1+\nu_m)]}{2(1+\nu_m)[E_m(1+V^{cnt})+2V_mp_r(1+\nu_m)]}, \tag{2.12}$$

$$m = \frac{E_m[E_mV_m+2m_r(1+\nu_m)(3+V^{cnt}-4\nu_m)]}{2(1+\nu_m)\{E_m[V_m+4V^{cnt}(1-\nu_m)]+2V_mm_r(3-\nu_m-4\nu_m^2)\}}, \tag{2.13}$$

in which k_r, l_r, n_r, m_r, and p_r are the equivalent Hill's elastic moduli of the reinforcing phase and can be determined from equality of the following matrices

$$C_r = \begin{bmatrix} n_r & l_r & l_r & 0 & 0 & 0 \\ l_r & k_r+m_r & k_r-m_r & 0 & 0 & 0 \\ l_r & k_r-m_r & k_r+m_r & 0 & 0 & 0 \\ 0 & 0 & 0 & m_r & 0 & 0 \\ 0 & 0 & 0 & 0 & p_r & 0 \\ 0 & 0 & 0 & 0 & 0 & p_r \end{bmatrix}, \tag{2.14}$$

$$C_r = \begin{bmatrix} \frac{1}{E_L} & -\frac{\nu_{TL}}{E_T} & -\frac{\nu_{ZL}}{E_Z} & 0 & 0 & 0 \\ -\frac{\nu_{LT}}{E_L} & \frac{1}{E_T} & -\frac{\nu_{ZT}}{E_Z} & 0 & 0 & 0 \\ -\frac{\nu_{LZ}}{E_L} & -\frac{\nu_{TZ}}{E_T} & \frac{1}{E_Z} & 0 & 0 & 0 \\ 0 & 0 & 0 & \frac{1}{G_{TZ}} & 0 & 0 \\ 0 & 0 & 0 & 0 & \frac{1}{G_{LZ}} & 0 \\ 0 & 0 & 0 & 0 & 0 & \frac{1}{G_{LT}} \end{bmatrix}^{-1} \tag{2.15}$$

where the engineering constants in Eq. (2.15) denote the corresponding material properties of the equivalent fiber. The subscripts L and (T, Z) refer to the directions parallel and normal to the fibers direction, respectively. Also, C_r is the tensor of elastic moduli of the reinforcing phase.

2.2.2. Composites reinforced with randomly oriented-straight CNTs. The orientation of the reinforcements in fiber reinforced composites significantly influences the effective material properties of such materials. In the case that CNTs are completely randomly oriented in the matrix, then the resulting composite is isotropic. Therefore, Young's modulus E and Poisson's ratio ν are evaluated as [35]

$$E = \frac{9KG}{3K+G}, \quad \nu = \frac{3K-2G}{6K+2G}, \tag{2.16}$$

where K and G are bulk modulus and shear modulus of the composite, respectively and can be stated as

$$\begin{aligned} K &= K_m + \frac{V^{cnt}(\delta_r - 3K_m\alpha_r)}{3(V_m + V^{cnt}\alpha_r)}, \\ G &= G_m + \frac{V^{cnt}(\eta_r - 2G_m\beta_r)}{2(V_m + V^{cnt}\beta_r)}, \end{aligned} \tag{2.17}$$

where

$$\alpha_r = \frac{3(K_m + G_m) + k_r - l_r}{3(G_m + k_r)}, \tag{2.18}$$

$$\begin{aligned} \beta_r = \frac{1}{5}\bigg\{ &\frac{4G_m + 2k_r + l_r}{3(G_m + k_r)} + \frac{4G_m}{G_m + p_r} \\ &+ \frac{2\left[G_m(3K_m + G_m) + G_m(3K_m + 7G_m)\right]}{G_m(3K_m + G_m) + m_r(3K_m + 7G_m)} \bigg\}, \end{aligned} \tag{2.19}$$

$$\delta_r = \frac{1}{3}\left[n_r + 2l_r + \frac{(2k_r + l_r)(3K_m + 2G_m - l_r)}{G_m + k_r} \right], \tag{2.20}$$

$$\begin{aligned} \eta_r = \frac{1}{5}\bigg[&\frac{2}{3}(n_r - l_r) + \frac{8G_m p_r}{G_m + p_r} + \frac{8m_r G_m(3K_m + 4G_m)}{3K_m(m_r + G_m) + G_m(7m_r + G_m)} \\ &+ \frac{2(k_r - l_r)(2G_m + l_r)}{3(G_m + k_r)} \bigg]. \end{aligned} \tag{2.21}$$

Also, K_m and G_m are the bulk and shear moduli of the isotropic matrix defined as

$$K_m = \frac{E_m}{3(1 - 2\nu_m)}, \quad G_m = \frac{E_m}{2(1 + \nu_m)}. \tag{2.22}$$

3. Theory and formulation

As shown in Fig. 2, a beam with the length of L, the width of b and the height of h is considered. The origin of the reference Cartesian coordinate system (x, y, z) is located in the center of the left plane of the beam while the x, y, and z axes are along the length, width and height directions of the beam, respectively. It is assumed that the FG-CNTRC beam is resting on a nonlinear viscoelastic foundation and subjected to a uniform harmonic transverse load to provide a more general problem. The displacement of an arbitrary point of the

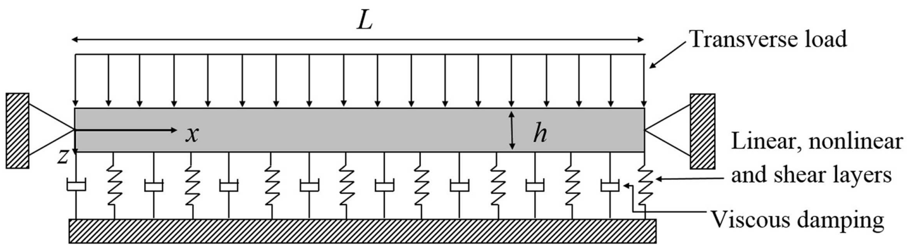

FIG. 2. Schematic view of FG-CNTRC beam with nonlinear viscoelastic foundation subjected to uniform transverse loading.

beam in the x and z directions can be expressed according to the Euler–Bernoulli beam theory as [21]

$$\widehat{U}(x,z,t) = U(x,t) - z\frac{\partial W(x,t)}{\partial x}, \quad \widehat{W}(x,z,t) = W(x,t), \tag{3.1}$$

in which U and W denote the axial and transverse displacement components in the mid-plane of the beam, respectively and t is the time. According to von Kármán assumptions, the normal stress can be determined as

$$\sigma_{xx} = Q_{11}(z)\left[\frac{\partial U}{\partial x} - z\frac{\partial^2 W}{\partial x^2} + \frac{1}{2}\left(\frac{\partial W}{\partial x}\right)^2\right], \tag{3.2}$$

where

$$Q_{11} = \frac{E_{11}(z)}{1 - \nu_{12}^2(z)}. \tag{3.3}$$

Based on Hamilton's principle, one can write

$$\int_0^{t_1} \delta(U_e - K - W_{ex})dt = 0, \tag{3.4}$$

where δ is the variational symbol. U_e and K are respectively the strain energy and kinetic energy evaluated as

$$U_e = \frac{b}{2}\int_0^L \int_{-h/2}^{h/2} Q_{11}(z)\left(\frac{\partial U}{\partial x} - z\frac{\partial^2 W}{\partial x^2} + \frac{1}{2}\left(\frac{\partial W}{\partial x}\right)^2\right)^2 dzdx, \tag{3.5}$$

$$K = \frac{b}{2}\int_0^L \int_{-h/2}^{h/2} \rho(z)\left[\left(\frac{\partial U}{\partial t}\right)^2 + \left(\frac{\partial W}{\partial t}\right)^2\right]dzdx. \tag{3.6}$$

Furthermore, W_{ex} refers to the work done by the external forces and it can be stated as follows

$$\delta W_{ext} = \int\limits_A P_{ex}(x,t)\delta W dA, \tag{3.7}$$

where P_{ex} is the summation of external forces per unit area of the beam which consists of the periodic transverse load and nonlinear foundation effect in the form of

$$P_{ex}(x,t) = F(x,t) - k_l W - k_{nl} W^3 + k_s \frac{\partial^2 W}{\partial x^2} - c\frac{\partial W}{\partial t}, \tag{3.8}$$

in which k_l, k_s, and k_{nl} are the linear, shear and nonlinear coefficients of the foundation and c is the viscous damping parameter. Also, $F(x,t)$ is the transverse harmonic force. By substituting the resulting equations of U_e, K and W_{ex} in the relation of Hamilton's principle, the equations of motion for the FG-CNTRC beams are derived as

$$\frac{\partial N_x}{\partial x} = I_1 \frac{\partial^2 U}{\partial t^2}, \tag{3.9}$$

$$\frac{\partial^2 M_x}{\partial x^2} + \frac{\partial}{\partial x}\left(N_x \frac{\partial W}{\partial x}\right) - k_l W - k_{nl} W^3 + k_s \frac{\partial^2 W}{\partial x^2} + F(x,t) = I_1 \frac{\partial^2 W}{\partial t^2} + c\frac{\partial W}{\partial t}. \tag{3.10}$$

Moreover, the related boundary conditions at the end points of the beam are derived as

$$N_x = 0 \quad \text{or} \quad \delta U = 0, \tag{3.11}$$

$$\frac{\partial M_x}{\partial x} + (k_s + N_x)\frac{\partial W}{\partial x} = 0 \quad \text{or} \quad \delta W = 0, \tag{3.12}$$

$$M_x = 0 \quad \text{or} \quad \delta\left(\frac{\partial W}{\partial x}\right) = 0. \tag{3.13}$$

In the above equations, M_x and N_x are the bending moment and normal force resultants respectively defined as

$$N_x = A_{11}\left[\frac{\partial U}{\partial x} + \frac{1}{2}\left(\frac{\partial W}{\partial x}\right)^2\right] - B_{11}\frac{\partial^2 W}{\partial x^2}, \tag{3.14}$$

$$M_x = B_{11}\left[\frac{\partial U}{\partial x} + \frac{1}{2}\left(\frac{\partial W}{\partial x}\right)^2\right] - D_{11}\frac{\partial^2 W}{\partial x^2}, \tag{3.15}$$

in which

$$\{A_{11}, B_{11}, D_{11}\} = \int_{-h/2}^{h/2} Q_{11}(z)\left\{1, z, z^2\right\} dz, \quad I_1 = \int_{-h/2}^{h/2} \rho(z) dz. \tag{3.16}$$

The axial inertia is assumed to be negligible, so Eq. (3.9) gives

$$\frac{\partial N_x}{\partial x} = 0 \quad \text{or} \quad N_x = \text{constant} = N_0. \tag{3.17}$$

Since the considered end supports of the beam are immovable (i.e. U =0 at x =0 and $x = L$), integration from (3.14) yields

$$N_0 = \frac{A_{11}}{L} \int_0^L \left[\frac{1}{2}\left(\frac{\partial W}{\partial x}\right)^2 - \frac{B_{11}}{A_{11}} \frac{\partial^2 W}{\partial x^2}\right] dx. \tag{3.18}$$

Moreover, the bending moment can be restated in terms of axial force resultant and transverse deflection as

$$M_x = \frac{B_{11}}{A_{11}}\left[N_0 + B_{11} \frac{\partial^2 W}{\partial x^2}\right] - D_{11} \frac{\partial^2 W}{\partial x^2}. \tag{3.19}$$

By substituting Eq. (3.19) into Eq. (3.10) and considering Eq. (3.17), the equations of motion of the beam reduce to one equation as

$$\left(\frac{B_{11}^2}{A_{11}} - D_{11}\right) \frac{\partial^4 W}{\partial x^4} + (N_0 + k_s) \frac{\partial^2 W}{\partial x^2} - k_l W - k_{nl} W^3 + F(x,t) = I_1 \frac{\partial^2 W}{\partial t^2} + c \frac{\partial W}{\partial t}. \tag{3.20}$$

For simplification and generality, the following dimensionless quantities are defined

$$\begin{aligned} &\zeta = \frac{x}{L}, \quad \bar{w} = \frac{W}{h}, \quad \eta = \frac{h}{L}, \quad \tau = \frac{t}{L}\sqrt{\frac{A_{110}}{I_{10}}}, \\ &(a_{11}, b_{11}, d_{11}) = \left(\frac{A_{11}}{A_{110}}, \frac{B_{11}}{A_{110} h}, \frac{D_{11}}{A_{110} h^2}\right), \quad \bar{I} = \frac{I_1}{I_{10}} \end{aligned} \tag{3.21}$$

where A_{110} and I_{10} are the values of A_{11} and I_1 of a homogenous beam made of the matrix material.

Using dimensionless parameters in Eq. (3.21), the dimensionless governing equation of the CNTRC beam can be obtained as

$$d_0 \eta^2 \frac{\partial^4 \bar{w}}{\partial \zeta^4} + (\bar{N}_0 + K_s) \frac{\partial^2 \bar{w}}{\partial \zeta^2} - K_l \bar{w} - K_{nl} \bar{w}^3 + \bar{F}(\zeta, \tau) = \bar{I} \frac{\partial^2 \bar{w}}{\partial \tau^2} + \bar{c} \frac{\partial \bar{w}}{\partial \tau}, \tag{3.22}$$

where $\bar{F}$ is the dimensionless transverse force. Also, K_l, K_s, K_{nl}, and $\bar{c}$ are the dimensionless parameters of the viscoelastic foundation. Other dimensionless parameters in addition to those explained in Eq. (3.21), are determined as

$$
\begin{aligned}
&K_l = \frac{L^2 k_l}{A_{110}}, && K_s = \frac{k_s}{A_{110}},\\
&K_{nl} = \frac{L^2 h^2 k_{nl}}{A_{110}}, && \bar{F} = \frac{F L^2}{h A_{110}},\\
&\bar{c} = \frac{cL}{\sqrt{A_{110} I_{10}}}, && d_0 = \frac{b_{11}^2}{a_{11}} - d_{11},\\
&\bar{N}_0 = a_{11}\eta^2 \int_0^1 \left[\frac{1}{2}\left(\frac{\partial \bar{w}}{\partial \zeta}\right)^2 - \frac{b_{11}}{a_{11}}\frac{\partial^2 \bar{w}}{\partial \zeta^2}\right] d\zeta.
\end{aligned}
\tag{3.23}
$$

According to the separation of variables analysis, the transverse displacement equation of the beam can be expressed as the multiplication of the mode shape function of the beam and an unknown time-dependent function.

$$\bar{w}(\zeta,\tau) = \phi(\zeta) w(\tau). \tag{3.24}$$

Table 1. Vibration mode shapes of beams for different boundary conditions.

Boundary conditions	Mode shape $\phi(\zeta)$	Coefficient β
S-S	$C_n \sin(\beta_n \zeta)$	$\beta_1 = \pi$ $\beta_2 = 2\pi$ $\beta_3 = 3\pi$
C-C	$D_n\left[\cosh(\beta_n\zeta) - \cos(\beta_n\zeta) - \frac{\cosh(\beta_n)-\cos(\beta_n)}{\sinh(\beta_n)-\sin(\beta_n)}(\sinh(\beta_n\zeta)-\sin(\beta_n\zeta))\right]$	$\beta_1 = 4.7300$ $\beta_2 = 7.8532$ $\beta_3 = 10.9956$
C-S	$Z_n\left[\cosh(\beta_n\zeta) - \cos(\beta_n\zeta) - \frac{\cosh(\beta_n)-\cos(\beta_n)}{\sinh(\beta_n)-\sin(\beta_n)}(\sinh(\beta_n\zeta)-\sin(\beta_n\zeta))\right]$	$\beta_1 = 3.9266$ $\beta_2 = 7.0686$ $\beta_3 = 10.2102$

where ϕ is the mode shape function given in Table 1 for different boundary conditions [42] and w is the time-dependent function which will be determined. In Table 1, the coefficients C_n, D_n, and Z_n are determined according to the maximum deflection of the beam. By Substituting Eq. (3.24) into Eq. (3.22) and applying Galerkin's technique, the governing equation takes the following form

$$\ddot{w} + \gamma_5 \dot{w} + (\gamma_1 + \alpha_1 + \alpha_2) w + \gamma_2 w^2 + (\gamma_3 + \alpha_3) w^3 = \gamma_4 \bar{F}, \tag{3.25}$$

where

$$
\begin{aligned}
&\gamma_1 = \frac{-d_0\eta^2 \int_0^1 \frac{d^4\phi}{d\zeta^4}\phi d\zeta}{\lambda_0}, \quad \gamma_2 = \frac{b_{11}\eta^2 \int_0^1 \frac{d^2\phi}{d\zeta^2}d\zeta \int_0^1 \frac{d^2\phi}{d\zeta^2}\phi d\zeta}{\lambda_0},\\
&\gamma_3 = \frac{-a_{11}\eta^2 \int_0^1 \left(\frac{d\phi}{d\zeta}\right)^2 d\zeta \int_0^1 \frac{d^2\phi}{d\zeta^2}\phi d\zeta}{2\lambda_0} \quad \gamma_4 = \frac{\int_0^1 \phi d\zeta}{\lambda_0}, \quad \gamma_5 = \frac{\bar{c}\int_0^1 \phi^2 d\zeta}{\lambda_0},\\
&\lambda_0 = \bar{I}\int_0^1 \phi^2 d\zeta, \quad \alpha_1 = \frac{K_l \int_0^1 \phi^2 d\zeta}{\lambda_0},\\
&\alpha_2 = \frac{-K_s \int_0^1 \frac{d^2\phi}{d\zeta^2}\phi d\zeta}{\lambda_0}, \quad \alpha_3 = \frac{K_{nl}\int_0^1 \phi^4 d\zeta}{\lambda_0}.
\end{aligned}
\tag{3.26}
$$

In this study, it is assumed that the beam is under the action of a distributed transverse harmonic load with the relation of

$$\bar{F} = f\cos(\Omega\tau) \tag{3.27}$$

in which f and Ω are dimensionless forms of the amplitude and frequency of the external excitation, respectively. Three types of end supports are considered for the beam, i.e., simply supported at both ends (S-S), clamped at both ends (C-C) and clamped at $x = 0$ and simply supported at $x = L$ (C-S), which must satisfy the following boundary conditions

• Simply supported-simply supported

$$\phi(0) = \phi(1) = 0, \quad \frac{d^2\phi(0)}{d\zeta^2} = \frac{d^2\phi(1)}{d\zeta^2} = 0. \tag{3.28}$$

• Clamped-clamped

$$\phi(0) = \phi(1) = 0, \quad \frac{d\phi(0)}{d\zeta} = \frac{d\phi(1)}{d\zeta} = 0. \tag{3.29}$$

• Clamped-simply supported

$$\phi(0) = \phi(1) = 0, \quad \frac{d\phi(0)}{d\zeta} = \frac{d^2\phi(1)}{d\zeta^2} = 0. \tag{3.30}$$

Also, the initial velocity and displacement for the forced vibration analysis of the FG-CNTRC beam are considered to be equal to zero.

4. Solution approach

In this study, the variational iteration method (VIM) is employed to solve the governing equation of forced vibration of the FG-CNTRC beams. The VIM presented by He [43] is a powerful and accurate analytical method wherein the approximations converge fast to the exact solution even in the case of highly nonlinear differential equations. Moreover, this technique provides closed form solutions which are helpful for parametric studies.

To demonstrate the principles of VIM, consider the following general nonlinear system [43]

$$Lu(t) + \varGamma u(t) = g(t). \tag{4.1}$$

In Eq. (4.1), L, $\varGamma$, and g represent the linear operator, nonlinear operator, and a real inhomogeneous term, respectively. The $(n+1)$th-order approximate solution of the differential equation can be determined by developing the following correction functional

$$u_{n+1}(t) = u_n(t) + \int_0^t \lambda(Lu_n(s) + \varGamma\tilde{u}_n(s) - g(s))ds \tag{4.2}$$

in which λ is a general Lagrange multiplier and can be found optimally using variational theory. Also, $\tilde{u}_n$ indicates a restricted variation, i.e. $\delta\tilde{u}_n = 0$.

4.1. Application of VIM in the forced vibration analysis

By introducing the following parameters, Eq. (3.25) can be simplified as

$$\begin{gathered}\ddot{w}(\tau) + \theta_5\dot{w}(\tau) + \theta_1 w(\tau) + \theta_2 w^2(\tau) + \theta_3 w^3(\tau) = \theta_4\cos(\varOmega\tau),\\ \theta_1 = \gamma_1 + \alpha_1 + \alpha_2, \quad \theta_2 = \gamma_2, \quad \theta_3 = \gamma_3 + \alpha_3, \quad \theta_4 = f\gamma_4, \quad \theta_5 = \gamma_5.\end{gathered} \tag{4.3}$$

The total solution of the above equation consists of the solutions of the steady state and the transient phases, which, respectively, are also called the particular solution, w_p, and the homogenous solution, w_h, i.e. $w(\tau) = w_p(\tau) + w_h(\tau)$. In the following, it is explained how both of the solutions are determined.

4.1.1. Steady state solution. To find the general Lagrange multiplier, Eq. (4.3) can be rewritten in the form of

$$\begin{gathered}\ddot{w} + \omega^2 w + Q(w, \dot{w}, \varOmega\tau) = 0,\\ Q(w, \dot{w}, \varOmega\tau) = \theta_1 w + \theta_2 w^2 + \theta_3 w^3 + \theta_5\dot{w} - \theta_4\cos(\varOmega\tau) - \omega^2 w,\end{gathered} \tag{4.4}$$

where Q is a function of w, $\dot{w}$ and $\Omega\tau$, and ω is the dimensionless natural frequency defined as

$$\omega = \bar{\omega} L \sqrt{\frac{I_{10}}{A_{110}}} \tag{4.5}$$

in which $\bar{\omega}$ is the dimensional natural frequency. Substitution of Eq. (4.4) into Eq. (4.2) yields

$$w_{n+1}(\tau) = w_n(\tau) + \int_0^\tau \lambda(s)[\ddot{w}_n(s) + \omega^2 w_n(s) + Q(\tilde{w}, \dot{\tilde{w}}, \Omega s)]ds. \tag{4.6}$$

By computing the variation of Eq. (4.6) with respect to w and utilizing integration by parts, the following stationary conditions are obtained

$$\frac{d^2\lambda(s)}{ds^2} + \omega^2\lambda(s) = 0, \quad 1 - \left.\frac{d\lambda(s)}{ds}\right|_{s=\tau} = 0, \quad \lambda(s=\tau) = 0. \tag{4.7}$$

Thus, the general Lagrange multiplier can be determined by solving the previous set of equations as

$$\lambda(s) = \frac{1}{\omega}\sin(\omega(s-\tau)). \tag{4.8}$$

According to the steady state solution of the linear forced vibration, the first approximation function is considered as

$$w_{p0}(\tau) = A\cos(\omega\tau + \psi) \tag{4.9}$$

where A and ψ are the dimensionless vibration amplitude ($w_{\max}$) and phase angle, respectively. It is worth noting that in the steady state phase of the forced vibration analysis, the vibration frequency is identical to the frequency of the external loading. Therefore, ω should be replaced with Ω. By substitution of Eqs. (4.3), (4.8) and (4.9) into Eq. (4.2), the first-order approximation can be written as

$$\begin{aligned} w_{p1} = {} & A\cos(\Omega\tau + \psi) + \int_0^\tau \frac{1}{\Omega}\sin(\Omega(s-\tau)) \\ & \times \left[\frac{1}{4}A^3\theta_3\cos(3\Omega s + 3\psi) + \frac{1}{2}A^2\theta_2\cos(2\Omega s + 2\psi) + \frac{1}{2}\theta_2 A^2\right]ds. \end{aligned} \tag{4.10}$$

Then, the first-order approximation of steady state phase of the time response is obtained by solving the above correction functional as follows,

$$w_{p1} = A\cos(\Omega\tau + \psi) + \frac{A^2}{96\Omega^2}(8\theta_2 H_1 + 3A\theta_3 H_2) \tag{4.11}$$

in which

$$
\begin{aligned}
H_1 &= 2\cos(2\Omega\tau+2\psi)-3\cos(\Omega\tau+2\psi)+\cos(-\Omega\tau+2\psi)+6\cos(\Omega\tau)-6,\\
H_2 &= \cos(3\Omega\tau+3\psi)-2\cos(\Omega\tau+3\psi)+\cos(-\Omega\tau+3\psi).
\end{aligned}
\tag{4.12}
$$

It should be remarked that in Eq. (4.10), the coefficients of $\cos(\Omega s)$ and $\sin(\Omega s)$ were equated to zero to avoid secular terms in the next iterations. Thus, a nonlinear system of equations is developed from which vibration amplitude, vibration frequency, and phase angle can be found

$$
\begin{aligned}
&\cos(\Omega s)\colon\ A\Omega^2\cos(\psi)+A\theta_5\Omega\sin(\psi)-\frac{3}{4}A^3\theta_3\cos(\psi)-A\theta_1\cos(\psi)+\theta_4=0,\\
&\sin(\Omega s)\colon\ A\Omega^2\sin(\psi)-A\theta_5\Omega\cos(\psi)-\frac{3}{4}A^3\theta_3\sin(\psi)-A\theta_1\sin(\psi)=0.
\end{aligned}
\tag{4.13}
$$

Moreover, the results of the next iterations can be calculated similarly. Also, by setting $\theta_4=\theta_5=\psi=0$ and repeating the same procedure, the nonlinear natural frequencies and time response of the undamped free vibration analysis of the beam is obtained.

4.1.2. Transient solution. In this section, it is assumed that the beam is not under the action of the external harmonic loading. Therefore, Eq. (4.3) is rewritten as

$$
\begin{aligned}
&\ddot{w}(\tau)+\theta_5\dot{w}(\tau)+\theta_1 w(\tau)+O(w)=0,\\
&O(w)=\theta_2 w^2+\theta_3 w^3.
\end{aligned}
\tag{4.14}
$$

Similar to the steady state solution, the corresponding stationary conditions for the general Lagrange multiplier are found via substituting Eq. (4.14) into (4.2) and evaluating the variation of the developed equation with respect to w and employing integration by parts as

$$
\begin{aligned}
&\frac{d^2\lambda(s)}{ds^2}-\theta_5\frac{d\lambda(s)}{ds}+\theta_1\lambda(s)=0,\\
&1-\left(\frac{d\lambda(s)}{ds}-\theta_5\lambda(s)\right)\Bigg|_{s=\tau}=0,\quad \lambda(s=\tau)=0.
\end{aligned}
\tag{4.15}
$$

Therefore, in this case, the Lagrange multiplier can be identified as

$$
\lambda(s)=\frac{1}{\mu}\sin(\mu(s-\tau))e^{\frac{\theta_5}{2}(s-\tau)}
\tag{4.16}
$$

where

$$
\mu=\sqrt{\theta_1-\left(\frac{\theta_5}{2}\right)^2}.
\tag{4.17}
$$

Based on the transient response of the linear forced vibration of the beam, the initial function is assumed to be in the form of

$$w_{h0}(\tau) = e^{-\frac{\theta_5}{2}\tau}(X\cos(\mu\tau) + Y\sin(\mu\tau)) \tag{4.18}$$

where X and Y are unknown constants which are determined according to the initial conditions. Substituting Eqs. (4.3), (4.16) and (4.18) into Eq. (4.2) and setting θ_4 =0 leads to the first-order approximation of the transient phase solution as

$$\begin{aligned} w_{h1} = \frac{1}{c_1}\Big\{ & e^{-\frac{\theta_5}{2}\tau}[(c_2 + c_1 Y)\sin(\mu\tau) + (c_3 + c_1 X)\cos(\mu\tau)] \\ & + e^{-\theta_5\tau}[c_4\sin(2\mu\tau) + c_5\cos(2\mu\tau) + c_6] \\ & + e^{-\frac{3\theta_5}{2}\tau}[c_7\sin(3\mu\tau) + c_8\cos(3\mu\tau) + c_9]\Big\} \end{aligned} \tag{4.19}$$

in which c_i $(i = 1, \ldots, 9)$ are evaluated through the relations presented in the Appendix. By repeating the same procedure, the higher-order approximations can be obtained. Thus, the nth-order solution of the full time history of the response of the FG-CNTRC beams on a nonlinear viscoelastic foundation is determined as

$$w_n = w_{pn} + w_{hn}. \tag{4.20}$$

5. Results and discussions

In this section, the numerical results for forced vibration frequencies and time response of the FG-CNTRC beams are presented. First of all, for authentication of the current approach, the corresponding solutions from the available references are provided for a comparative study. The nonlinear free vibration

Table 2. Nonlinear free vibration frequency ratios (ω_{nl}/ω_l) for S-S and C-C isotropic beams.

	$W_{\max}/\sqrt{I/S}$	1st App.	2nd App.	3rd App.	Ref. [44]	Ref. [45]
S-S	0.5	1.0232	1.0231	1.0231	–	1.0231
	1	1.0897	1.0892	1.0892	1.0892	1.0892
	2	1.3229	1.3180	1.3178	1.3178	1.3178
	3	1.6394	1.6263	1.6257	1.6257	1.6257
C-C	0.5	1.0056	1.0056	1.0056	–	1.0056
	1	1.0222	1.0222	1.0222	1.0222	1.0222
	2	1.0862	1.0857	1.0857	1.0857	1.0857
	3	1.1852	1.1832	1.1831	1.1831	1.1831

frequency ratios (ω_{nl}/ω_l) of isotropic homogeneous beams with S-S and C-C boundary conditions based on the first three iterations of the VIM are given in Table 2. It can be seen that the results agree very well with those calculated using the harmonic balance method (HBM) [44] and the direct numerical integration solution [45]. Furthermore, the fast rate of convergence of the method is noticeable. Here, $W_{\max}$, I and S refer to the dimensional maximum transverse deflection, area moment of inertia and cross-sectional area of the beam, respectively. In Table 3, the calculated values of the frequency ratios (Ω/ω_l) for undamped nonlinear forced vibration of S-S isotropic beams subjected to a uniform harmonic distributed excitation are compared with the counterparts reported by other references [44,46] and as observed, a good agreement is achieved again.

Table 3. Frequency ratios (Ω/ω_1) for undamped nonlinear forced vibration of S-S isotropic beams with $\sqrt{12}\gamma_4 = 2$.

$W_{\max}/\sqrt{I/S}$	1st App.	2nd App.	HBM [44]	Elliptic solution [46]
2	0.8660	0.8181	0.8660	0.8472
3	1.4216	1.3925	1.4216	1.4003
4	1.8708	1.8379	1.8708	1.8413
5	2.2995	2.2596	2.2995	2.2606

Figure 3 plots the damped free vibration time response of a beam with $\theta_1 = 20$, $\theta_2 = 0$, $\theta_3 = 2$, $\theta_5 = 1$, $w(0) = -0.2$ and $\dot{w}(0) = 2$. It is found that the present curve exhibits excellent agreement with the one presented by Nourazar and Mirzabeygi [47] wherein the modified differential transform

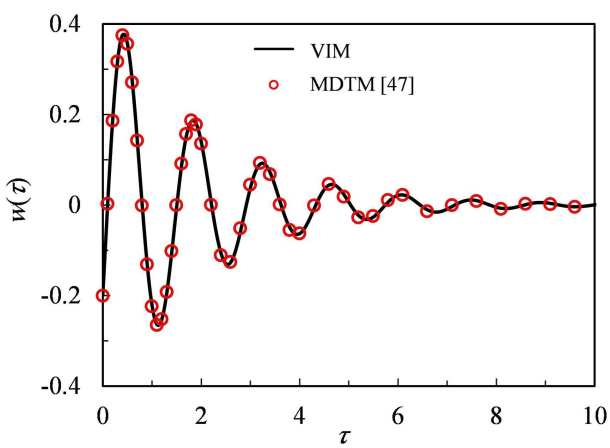

Fig. 3. Comparison of the damped free vibration time response of beams using VIM and MDTM [47].

method (MDTM) is used to solve the homogeneous damped Duffing equation. The accuracy of the presented EMT approach is illustrated in Fig. 4. The nonlinear free vibration frequencies of a C-S FGA-CNTRC beam reinforced with aligned-straight CNTs assessed by EMT method are compared to those calculated using ERM [21]. In Fig. 4, Poly methyl methacrylate (PMMA) and $(10, 10)$ SWCNTs are considered as the matrix and reinforcements, respectively. It can be deduced from Fig. 4 that there is a good agreement between the results which confirms the correctness of the applied EMT technique.

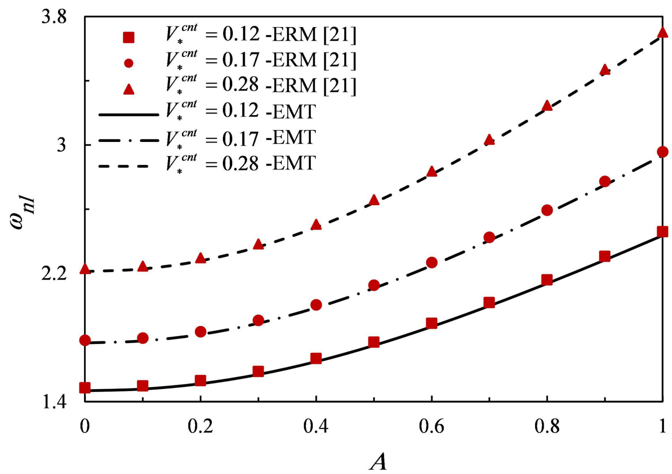

FIG. 4. Dimensionless frequencies of nonlinear free vibration for C-S FGA-CNTRC beams reinforced with aligned-straight CNTs ($L/h = 15$).

At the next stage, the effects of different parameters on the vibration frequencies and time response of the FG-CNTRC beams are investigated. In this study, PMMA with the material properties of $E_m = 2.5$ GPa, $\nu_m = 0.3$ and $\rho_m = 1190$ kg/m^3 at room temperature is considered as the matrix material. The selected reinforcements are armchair (10,10) SWCNTs. The corresponding material properties are assumed to be $E_{11}^{cnt} = 5.6466$ TPa, $E_{22}^{cnt} = 7.0800$ TPa, $G_{12}^{cnt} = 1.9445$ TPa, $\nu_{12}^{cnt} = 0.175$ and $\rho^{cnt} = 1400$ kg/m^3 with the effective wall thickness of 0.067 nm [36]. For ERM method, the CNT efficiency parameters are evaluated via matching the values of elastic modulus obtained from MD simulations [16] with the ones predicted through ERM as [36]:

$$\begin{aligned}
V_*^{cnt} &= 0.12: \quad \eta_1 = 0.137,\ \eta_2 = 1.022,\ \eta_3 = 0.715,\\
V_*^{cnt} &= 0.17: \quad \eta_1 = 0.142,\ \eta_2 = 1.626,\ \eta_3 = 1.138,\\
V_*^{cnt} &= 0.28: \quad \eta_1 = 0.141,\ \eta_2 = 1.585,\ \eta_3 = 1.109.
\end{aligned}$$

All of the forced vibration results are calculated for FGA-CNTRC beams with randomly oriented-straight CNTs as reinforcements and the slenderness ratio of

L/h =30, unless otherwise stated. It should be also mentioned that since the steady state phase is significantly more important than the transient phase in the forced vibration analysis, the vibration amplitude of the steady state phase is used in Figs. 5 to 10.

Table 4. Dimensionless natural frequencies (ω_{nl}) for nonlinear free vibration of S-S CNTRC beams based on the ERM and EMT approaches ($V_*^{cnt} = 0.12$).

A	UD-CNTRC			FGA-CNTRC			FGX-CNTRC			FGO-CNTRC		
	ERM	EMT		ERM	EMT		ERM	EMT		ERM	EMT	
		Aligned CNTs	Oriented CNTs		Aligned CNTs	Oriented CNTs		Aligned CNTs	Oriented CNTs		Aligned CNTs	Oriented CNTs
0	0.5766	0.5710	0.2625	0.4768	0.4699	0.2287	0.7012	0.6952	0.3246	0.4135	0.4075	0.1957
0.5	0.7189	0.7119	0.3273	0.6512	0.6430	0.3074	0.8223	0.8149	0.3809	0.5946	0.5874	0.2786
1	1.0296	1.0196	0.4687	1.0467	1.0357	0.4879	1.1044	1.0940	0.5119	0.9449	0.9346	0.4401
1.5	1.4000	1.3864	0.6373	1.4622	1.4476	0.6795	1.4555	1.4414	0.6749	1.3375	1.3236	0.6217
2	1.7939	1.7765	0.8167	1.8814	1.8629	0.8732	1.8368	1.8188	0.8518	1.7444	1.7265	0.8102

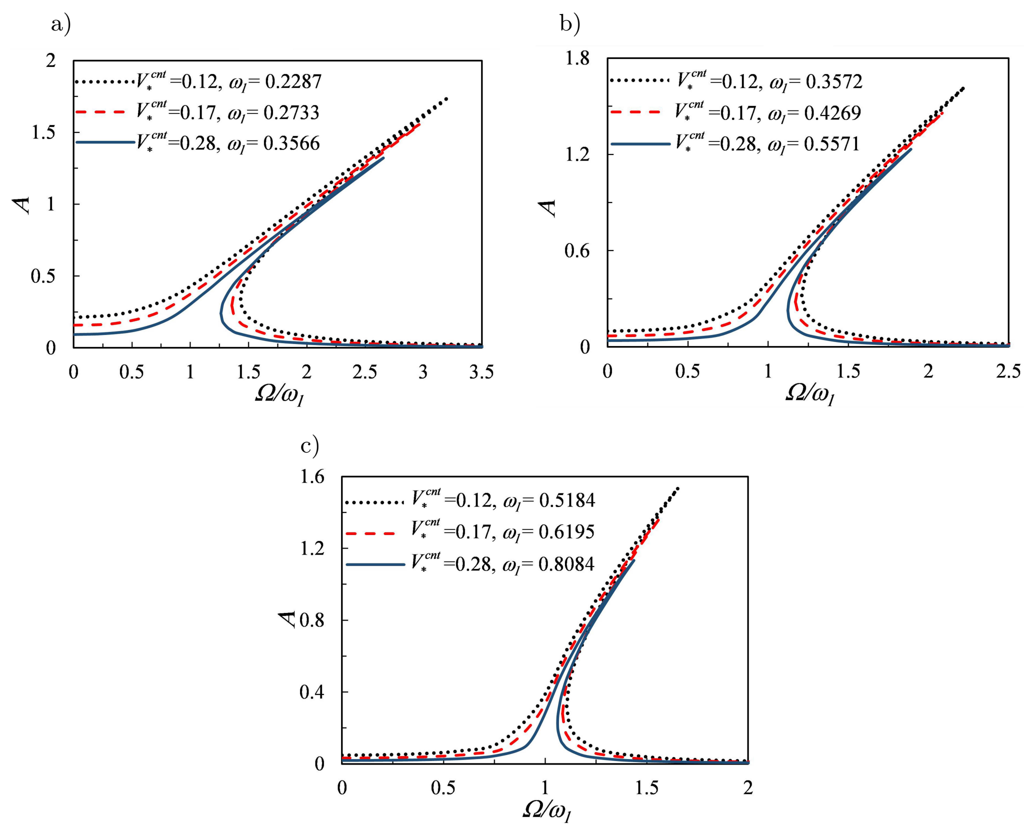

Fig. 5. Frequency ratio (Ω/ω_l) versus amplitude for nonlinear forced vibration of FGA-CNTRC beams with different volume fractions and end conditions; a) S-S, b) C-S, and c) C-C ($f = 0.01$, $\bar{c} = 0.01$).

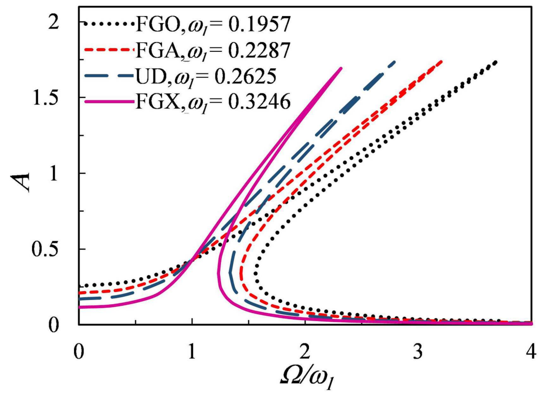

Fig. 6. Frequency ratio (Ω/ω_l) versus amplitude for nonlinear forced vibration of S-S FG-CNTRC beams with different CNT distributions ($V_*^{cnt} = 0.12$, $f = 0.01$, $\bar{c} = 0.014$).

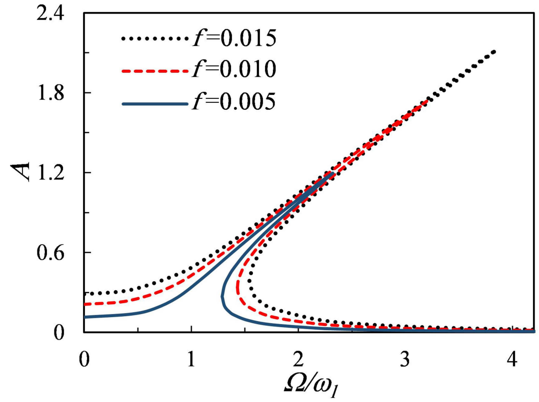

Fig. 7. Nonlinear forced vibration frequency response for S-S FGA-CNTRC beams with different values of dimensionless force amplitudes ($V_*^{cnt} = 0.12$, $\bar{c} = 0.01$).

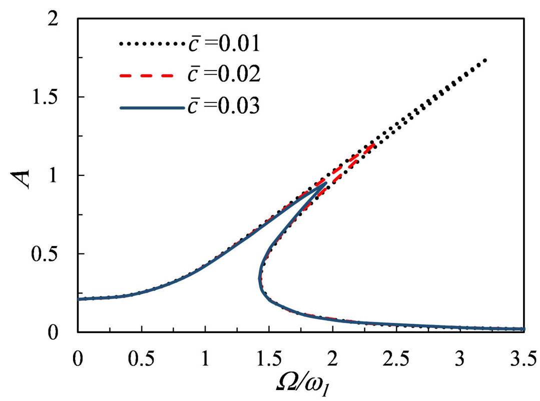

Fig. 8. Nonlinear forced vibration frequency response for S-S FGA-CNTRC beams with different values of dimensionless damping coefficients ($V_*^{cnt} = 0.12$, $f = 0.01$).

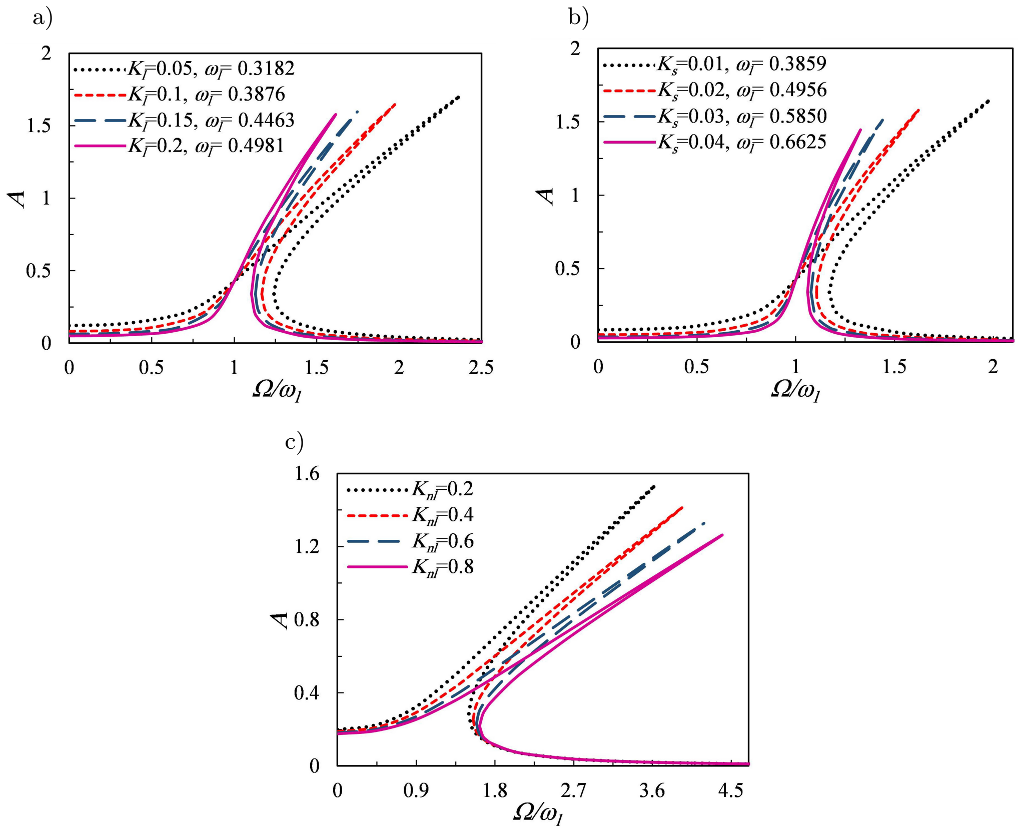

Fig. 9. Nonlinear forced vibration frequency response for S-S FGA-CNTRC beams with different values of elastic foundation parameters ($V_*^{cnt} = 0.12$, $f = 0.01$, $\bar{c} = 0.01$); a) K_l ($K_s = K_{nl} = 0$), b) K_s ($K_l = K_{nl} = 0$), c) K_{nl} ($K_l = K_s = 0$).

The effect of orientation of the CNTs on the dimensionless natural frequencies for nonlinear free vibration of S-S CNTRC beams with V_*^{cnt} =0.12 is demonstrated in Table 4. It can be seen that the values of frequencies for beams reinforced with aligned-straight CNTs based on the ERM and EMT methods are almost the same and more than those of randomly oriented CNT-reinforced beams. Also, it is found that increasing the vibration amplitude enhances the dimensionless natural frequencies. Figure 5 depicts the variations of frequency ratio (Ω/ω_l) in terms of dimensionless amplitude for the forced vibration of S-S, C-C and C-S FGA-CNTRC beams with different volume fractions. As shown, the vibration amplitude peak decreases by increasing the CNTs volume fraction. It can be also concluded that S-S beams have the greatest value of vibration amplitude peak which is followed by C-S and C-C boundary conditions, respectively. Furthermore, it is readily seen that the S-S beam frequency response curve

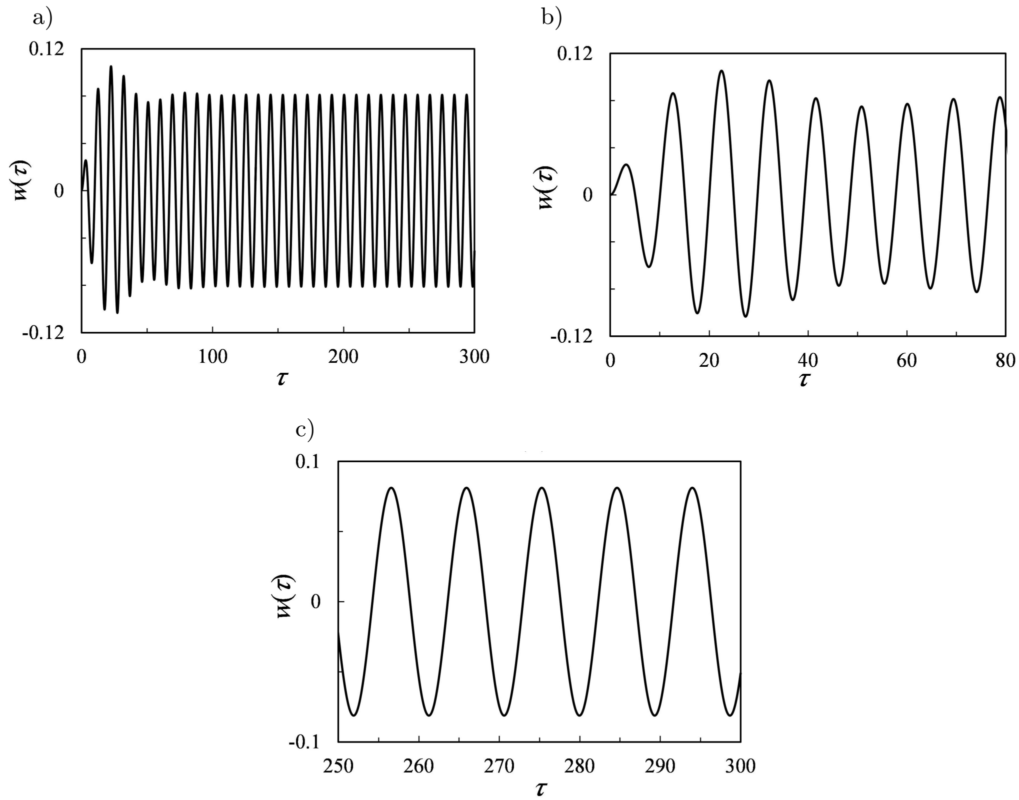

Fig. 10. Time response of S-S FGX-CNTRC beams ($V_*^{cnt} = 0.28$, $f = 0.01$, $\bar{c} = 0.1$, $\Omega = 1.2\omega_l$); a) full-time history, b) transient phase, c) steady state phase.

has the most deviation to the right side. This is due to the nonlinear nature of the problem, i.e. the beam with the highest nonlinearity in its behavior has the most leaning. Figure 6 illustrates the influence of CNTs distribution patterns on the forced vibration frequency response of S-S FG-CNTRC beams. The results reveal that FGO and FGX distributions possess the highest and lowest values of maximum amplitude peak, respectively. It is also found that the least deviation belongs to the beam with the stiffest CNT distribution pattern.

The effects of dimensionless force amplitude on the forced vibration frequency response of FGA-CNTRC beams are investigated in Fig. 7. As observed, enhancing the force amplitude increases the vibration amplitude peak. Figs. 8 and 9 exhibit the effects of nonlinear viscoelastic foundation parameters on the nonlinear forced vibration frequency response of the CNTRC beams. It can be noticed that the highest amplitude peak belongs to the beam with the lowest damping coefficient. It is also found that the variation of damping coefficient only changes the maximum amount of the amplitude. The linear and shear coefficients of the foundation have similar effects on the maximum amplitude peak while enhancing these coefficients yields to the reduction of the amplitude. Also, by increasing the linear and shear parameters, the effect of nonlinear coefficient of the foundation is diminished and accordingly, the leaning of the frequency response curve is decreased. On the other hand, although magnifying the nonlinear coefficient of the foundation reduces the amplitude peak as well, however, it increases the nonlinear stiffness of the foundation and results in bending of the curve to the right side. One more conclusion is that by increasing the values of the foundation parameters, the stiffness of the beam enhances and subsequently, the effect of the foundation on the frequency response of the beam decreases. The forced vibration time response of S-S FGX-CNTRC beams under the action of an external distributed harmonic excitation is plotted in Fig. 10. It is observed that in the transient phase, the beam oscillates irregularly, but in the steady state phase, the vibration amplitude remains constant. Also, the steady state response of the beam is independent of the initial conditions.

6. Conclusions

In this work, the analytical solutions for the frequency and time response of nonlinear forced vibration of FG-CNTRC beams are presented. It is assumed that the beam is subjected to a transverse harmonic load and resting on a nonlinear viscoelastic foundation. The aligned- or randomly oriented-straight CNTs in a polymeric matrix are considered as the reinforcements of the beams. The material properties of the beam are graded through the thickness direction with different distribution patterns and both the extended rule of mixture and Eshelby–Mori–Tanka approaches are utilized to predict the effective material properties. The governing equation of motion of the FG-CNTRC beams is derived via Euler–Bernoulli beam theory in conjunction with Hamilton's principle and von Kármán strain-displacement relations. Using the variational iteration method, the governing equation is solved and closed form expressions for forced vibration frequency and time responses of the nanocomposite beam are provided. The correctness of the current procedure is established through comparing the present results with those available in the literature. According to the developed analytical solutions, a parametric study is conducted to examine the influence of different parameters such as CNTs distribution, CNTs volume fraction, CNTs orientation, vibration amplitude, boundary conditions, the external excitation amplitude and the foundation coefficients on the vibrational properties of the FG-CNTRC beams. The results reveal that enhancing the CNTs volume fraction or the viscoelastic foundation parameters decreases the maximum amplitude peak. It is also found that increasing the external force amplitude results in larger amplitude peaks. Furthermore, the FGO distribution of CNTs possesses the highest amplitude peak.

Appendix

$$c_1 = 8\mu^2\theta_5(\theta_5^2 + 4\mu^2)(\theta_5^2 + 16\mu^2)(\theta_5^2 + 36\mu^2) \tag{A.1}$$

$$\begin{aligned} c_2 = &-8\mu(\theta_5^2 + 16\mu^2)\big\{X^2(X\theta_3 + 2\theta_2)\theta_5^4 + \mu XY(3X\theta_3 + 8\theta_2)\theta_5^3 \\ &+ 2\mu^2\big[3X\theta_3(6X^2 + Y^2) + 4\theta_2(7X^2 + 2Y^2)\big]\theta_5^2 \\ &+ 6Y\mu^3(Y^2\theta_3 + 15\theta_3X^2 + 16\theta_2X)\theta_5 \\ &+ 24X\mu^4\theta_3(6Y^2 + X^2)\big\} + 960Y\mu^6\theta_3\theta_5(3X^2 - Y^2) \\ &+ 3840X\mu^7\theta_3(3Y^2 - X^2) \\ &+ Y\theta_5(\theta_5^2 + 4\mu^2)(\theta_5^2 + 16\mu^2)(\theta_5^2 + 36\mu^2)(4\mu^2 - 4\theta_1 + \theta_5^2) \\ &+ X\mu\theta_5(\theta_5^2 + 4\mu^2)(\theta_5^2 + 16\mu^2)(\theta_5^2 + 36\mu^2)(4\mu^2 - 4\theta_1 + \theta_5^2)\tau, \end{aligned} \tag{A.2}$$

$$\begin{aligned} c_3 = &\,8\mu^2(\theta_5^2 + 16\mu^2)\big\{X^2(X\theta_3 + 2\theta_2)\theta_5^3 + 2\mu XY(3X\theta_3 + 16\theta_2)\theta_5^2 \\ &+ 6\mu^2\big[X\theta_3(5X^2 + 3Y^2) + 8\theta_2(X^2 + 2Y^2)\big]\theta_5 \\ &+ 24Y\mu^3\theta_3(6X^2 + Y^2)\big\} - 960X\mu^6\theta_3(X^2 - 3Y^2) \\ &- 3840Y\mu^7\theta_3(3X^2 - Y^2) \\ &- Y\mu\theta_5(\theta_5^2 + 4\mu^2)(\theta_5^2 + 16\mu^2)(\theta_5^2 + 36\mu^2)(4\mu^2 - 4\theta_1 + \theta_5^2)\tau, \end{aligned} \tag{A.3}$$

$$c_4 = 32\mu^2\theta_2\theta_5(\theta_5^2 + 16\mu^2)\big[XY(12\mu^2 - \theta_5^2) + 4\mu\theta_5(X^2 - Y^2)\big], \tag{A.4}$$

$$c_5 = 16\mu^2\theta_2\theta_5(\theta_5^2 + 16\mu^2)\big[(12\mu^2 - \theta_5^2)(X^2 - Y^2) - 16XY\mu\theta_5\big], \tag{A.5}$$

$$c_6 = -16\mu^2\theta_2\theta_5(\theta_5^2 + 16\mu^2)(\theta_5^2 + 36\mu^2)(X^2 + Y^2), \tag{A.6}$$

$$\begin{aligned} c_7 = &\,2\mu^2\theta_3\theta_5(\theta_5^2 + 36\mu^2) \\ &\times \big[Y(Y^2 - 3X^2)(\theta_5^2 - 8\mu^2) + 6X\mu\theta_5(X^2 - 3Y^2)\big], \end{aligned} \tag{A.7}$$

$$\begin{aligned} c_8 = &\,2\mu^2\theta_3\theta_5(\theta_5^2 + 36\mu^2) \\ &\times \big[-X(X^2 - 3Y^2)(\theta_5^2 - 8\mu^2) + 6Y\mu\theta_5(Y^2 - 3X^2)\big], \end{aligned} \tag{A.8}$$

$$\begin{aligned} c_9 = &\,6\mu^2\theta_3(\theta_5^2 + 16\mu^2)(\theta_5^2 + 36\mu^2)(X^2 + Y^2) \\ &\times \big[2\mu(X - Y) - \theta_5(X + Y)\big]. \end{aligned} \tag{A.9}$$

References

1. M. Yamanouchi, M. Koizumi, T. Hirai, I. Shiota (Eds.), *Proceedings of the First International Symposium on Functionally Gradient Materials*, Functionally Gradient Materials Forum, Sendai, Japan, 1990.

2. M. Koizumi, M. Niino, *Overview of FGM research in Japan*, MRS Bulletin, **20**, 19–21, 1995.

3. M.N.M. Allam, R. Tantawy, A.M. Zenkour, *Thermoelastic stresses in functionally graded rotating annular disks with variable thickness*, Journal of Theoretical and Applied Mechanics, **56**, 1029–1041, 2018.

4. A. Gupta, M. Talha, *Recent development in modeling and analysis of functionally graded materials and structures*, Progress in Aerospace Sciences, **79**, 1–14, 2015.

5. P.T. Thang, T.N. Thoi, J. Lee, *Mechanical stability of metal foam cylindrical shells with various porosity distributions*, Mechanics of Advanced Materials and Structures, 1–9, 2018. https://doi.org/10.1080/15376494.2018.1472338.

6. H.S. Shen, *Functionally Graded Materials*, *Nonlinear Analysis of Plates and Shells*, CRC Press, New York, 2016.

7. J. Fariborz, R.C. Batra, *Free vibration of bi-directional functionally graded material circular beams using shear deformation theory employing logarithmic function of radius*, Composite Structures, **210**, 217–230, 2019.

8. L.C. Trinh, T.P. Vo, H.T. Thai, T.K. Nguyen, *An analytical method for the vibration and buckling of functionally graded beams under mechanical and thermal loads*, Composites Part B: Engineering, **100**, 152–163, 2016.

9. N.I. Kim, T.A. Huynh, Q.X. Lieu, J. Lee, *NURBS-based optimization of natural frequencies for bidirectional functionally graded beams*, Archives of Mechanics, **70**, 337–364, 2018.

10. A.G. Shenas, S. Ziaee, P. Malekzadeh, *Nonlinear vibration analysis of pre-twisted functionally graded microbeams in thermal environment*, Thin-Walled Structures, **118**, 87–104, 2017.

11. S. Iijima, *Helical microtubules of graphitic carbon*, Nature, **354**, 56–58, 1991.

12. I.R. Pavlovic, R. Pavlovic, G. Janevski, *Mathematical modeling and stochastic stability analysis of viscoelastic nanobeams using higher-order nonlocal strain gradient theory*, Archives of Mechanics, **71**, 137–153, 2019.

13. R. Hosseini-Ara, *Nano-scale effects on nonlocal boundary conditions for exact buckling analysis of nano-beams with different end conditions*, Journal of Brazilian Society of Mechanical Sciences and Engineering, **40**, 144, 2018.

14. A.R. Setoodeh, H. Badjian, *Mechanical behavior enhancement of defective graphene sheet employing boron nitride coating via atomistic study*, Materials Research Express, 2017, https://doi.org/10.1088/2053-1591/aa9ac2.

15. V. Mittal, *Polymer Nanotube Nanocomposites*, *Synthesis, Properties and Applications*, John Wiley and Sons, New Jersey, 2010.

16. Y. Han, J. Elliot, *Molecular dynamics simulations of the elastic properties of polymer/carbon nanotube composites*, Computational Materials Science, **39**, 315–323, 2007.

17. D.G. Ninh, *Nonlinear thermal torsional post-buckling of carbon nanotube-reinforced composite cylindrical shell with piezoelectric actuator layers surrounded by elastic medium*, Thin-Walled Structures, **123**, 528–538, 2018.

18. H. Shafiei, A.R. Setoodeh, *Buckling and post-buckling analysis of FG-CNTRC beams: An exact closed form solution*, Journal of Aerospace Science and Technology, **11**, 33–41, 2017.

19. P.T. Thang, T.N. Thoi, J. Lee, *Closed-form solution for nonlinear buckling analysis of FG-CNTRC cylindrical shells with initial geometric imperfections*, European Journal of Mechanics- A/Solids, **73**, 483–491, 2019.

20. A.R. Setoodeh, M. Shojaee, *Critical buckling load optimization of functionally graded carbon nanotube-reinforced laminated composite quadrilateral plates*, Polymer Composites, 2017. http://dx.doi.org/10.1002/pc.24289.

21. H. Shafiei, A.R. Setoodeh, *Nonlinear free vibration and post-buckling of FG-CNTRC beams on nonlinear foundation*, Steel and Composite Structures, **24**, 65–77, 2017.

22. R. Zhong, Q. Wang, J. Tang, C. Shuai, B. Qin, *Vibration analysis of functionally graded carbon nanotube reinforced composites (FG-CNTRC) circular, annular and sector plates*, Composite Structures, **194**, 49–67, 2018.

23. N.D. Duc, J. Lee, T.N. Thoi, P.T. Thang, *Static response and free vibration of functionally graded carbon nanotube-reinforced composite rectangular plates resting on Winkler-Pasternak elastic foundations*, Aerospace Science and Technology, **68**, 391–402, 2017.

24. P. Malekzadeh, A.R. Zarei, *Free vibration of quadrilateral laminated plates with carbon nanotube reinforced composite layers*, Thin-Walled Structures, **82**, 221–232, 2014.

25. Y.H. Yas, N. Samadi, *Free vibration and buckling analysis of carbon nanotube-reinforced composite Timoshenko beams on elastic foundation*, International Journal of Pressure Vessels and Piping, **98**, 119–128, 2012.

26. H.L. Wu, J. Yang, S. Kitipornchai, *Nonlinear vibration of functionally graded carbon nanotube-reinforced composite beams with geometric imperfections*, Composites Part B: Engineering, **90**, 86–96, 2016.

27. A.G. Shenas, P. Malekzadeh, S. Ziaee, *Vibration analysis of pre-twisted functionally graded carbon nanotube reinforced composite beams in thermal environment*, Composite Structures, **162**, 325–340, 2017.

28. T. Vo-Duy, V. Ho-Huu, T. Nguyen-Thoi, *Free vibration analysis of laminated FG-CNT reinforced composite beams using finite element method*, Frontiers of Structural and Civil Engineering, **13**, 324–336, 2019.

29. M.H. Yas, M. Heshmati, *Dynamic analysis of functionally graded nanocomposite beams reinforced by randomly oriented carbon nanotube under the action of moving load*, Applied Mathematical Modelling, **36**, 1371–1394, 2012.

30. R. Ansari, M. Faghih Shojaei, V. Mohammadi, R. Gholami, F. Sadeghi, *Nonlinear forced vibration analysis of functionally graded carbon nanotube-reinforced composite Timoshenko beams*, Composite Structures, **113**, 316–327, 2014.

31. Z. Wu, Y. Zhang, G. Yao, Z. Yang, *Nonlinear primary and super-harmonic resonances of functionally graded carbon nanotube reinforced composite beams*, International Journal of Mechanical Sciences, **153-154**, 321–340, 2019.

32. D. Younesian, A. Hosseinkhani, H. Askari, E. Esmailzadeh, *Elastic and viscoelastic foundations: a review on linear and nonlinear vibration modeling and applications*, Nonlinear Dynamics, 1–43, 2019.

33. Y.H. Chen, Y.H. Huang, C.T. Shih, *Response of an infinite Timoshenko beam on a viscoelastic foundation to a harmonic moving load*, Journal of Sound and Vibration, **241**, 809–824, 2001.

34. U. Bhattiprolu, A.K. Bajaj, P. Davies, *Effect of axial load on the response of beams on nonlinear viscoelastic unilateral foundations*, ASME 2014 International Design Engi-

neering Technical Conferences and Computers and Information in Engineering Conference, American Society of Mechanical Engineers Digital Collection, 2014.

35. D.L. Shi, X.Q. Feng, Y.Y. Huang, K.C. Hwang, H. Gao, *The effect of nanotube waviness and agglomeration on the elastic property of carbon nanotube-reinforced composites*, Journal of Engineering Materials and Technology, **126**, 250–257, 2004.

36. H.S. Shen, C.L. Zhang, *Thermal buckling and postbuckling behavior of functionally graded carbon nanotube-reinforced composite plates*, Materials & Design, **31**, 3403–3411, 2010.

37. C.H. Chen, C.H. Cheng, *Effective elastic moduli of misoriented short-fiber composites*, International Journal of Solids and Structures, **33**, 2519–2539, 1996.

38. G.M. Odegard, T.S. Gates, K.E. Wise, C. Park, E.J. Siochi, *Constitutive modeling of nanotube-reinforced polymer composites*, Composites Science and Technology, **63**, 1671–1687, 2003.

39. T. Mori, K. Tanaka, *Average stress in matrix and average elastic energy of materials with misfitting inclusions*, Acta Metallurgica, **21**, 571–574, 1973.

40. J.D. Eshelby, *The determination of the elastic field of an ellipsoidal inclusion, and related problems*, Proceedings of the Royal Society of London A: Mathematical, Physical and Engineering Sciences, **241**, 376–396, 1957.

41. E. Garcia-Macias, L. Rodriguez-Tembleque, R. Castro-Triguero, A. Saez, *Buckling analysis of functionally graded carbon nanotube-reinforced curved panels under axial compression and shear*, Composites Part B: Engineering, **108**, 243–256, 2017.

42. S.S. Rao, *Vibration of Continuous Systems*, John Wiley and Sons, New Jersey, 2007.

43. J.H. He, *Variational iteration method- a kind of non-linear analytical technique: some examples*, International Journal of Non-Linear Mechanics, **34**, 699–708, 1999.

44. L. Azrar, R. Benamar, R.G. White, *Semi-analytical approach to the nonlinear dynamic response problem of S-S and C-C beams at large vibration amplitudes, part I: General theory and application to the single mode approach to free and forced vibration analysis*, Journal of Sound and Vibration, **224**, 183–207, 1999.

45. L.L. Ke, J. Yang, S. Kitipornchai, *An analytical study on the nonlinear vibration of functionally graded beams,* Meccanica, **45**, 743–752, 2010.

46. C. Mei, K. Decha-Umphai, *A finite element method for non-linear forced vibrations of beams*, Journal of Sound and Vibration, **102**, 369–380, 1985.

47. S. Nourazar, A. Mirzabeigy, *Approximate solution for nonlinear Duffing oscillator with damping effect using the modified differential transform method*, Scientia Iranica, **20**, 364–368, 2013.

Received May 10, 2019; revised version April 7, 2020.
Published online April 30, 2020.